

Green's functions in thermal-wave physics: Cartesian coordinate representations

Andreas Mandelis^{a)}

Photothermal and Optoelectronic Diagnostics Laboratory and Manufacturing Research Corporation of Ontario, University of Toronto, Toronto M5S 1A4, Canada

(Received 15 June 1994; accepted for publication 16 March 1995)

A self-consistent integral formulation of Green's functions in thermal wave-physics is presented in one, two, and three dimensions and for infinite, semi-infinite, and spatially bounded geometries. Furthermore, several applications are explicitly worked out based on either Dirichlet or Neumann boundary conditions and resulting in well-known or novel integral expressions for propagating thermal-wave fields in thermally homogeneous media and in experimentally useful geometries. It is hoped that the Green's functions methodologies will enhance their use by investigators who wish to take advantage of their elegance, mathematical simplicity, and computational power. © 1995 American Institute of Physics.

I. INTRODUCTION

Thermal waves are used extensively for nondestructive evaluation, subsurface defect imaging, depth profilometry, and tomography.^{1,2} In all of these applications, detection of inhomogeneities and defect structures is based on the scattering of thermal waves, which is ultimately the result of local variations in the thermal diffusivity. It is well known that scatterer detection methodologies using propagating fields (e.g., acoustic, electromagnetic, optical, microwave) can best be quantified using Green's function techniques, because detailed knowledge of the distribution of the object (field) function inside a spatial region can be reconstructed by detailed knowledge of the field values on the boundaries surrounding the spatial region (volume). This important consequence of Green's Theorem³ can be put in straightforward mathematical terms by use of Green's functions appropriate for specific geometries. The advantage of Green's function formalisms is, of course, that the function itself is the representation of a field response to an impulsive source in space or time, or both, which is the simplest kind of source. Subsequently, the field response to any arbitrary source distribution can be represented as a convolution integral of the distribution with Green's function over the source coordinates.

In the analytical theory of heat diffusion Green's function techniques have been utilized for some time⁴ with wide-ranging applications to problems in conduction heat transfer.⁵ These problems are transient (time-domain) formulations and have found recent applications in photothermal systems using pulsed excitation (Ref. 2, Chap. 2, and Ref. 6) or impulse-response spectral correlation analysis.⁷ The development of Green's function methodologies is by no means as advanced in the frequency-domain conduction heat transfer analysis, otherwise known as "thermal waves." The reasons are mainly two: the absence of pre-existing Green's function formalisms in this area in widely accepted "classic" books and treatises such as those by Carslaw and Jaeger⁵ or Arpacı,⁸ (such older monographs have not dealt with the thermal-wave field extensively, most likely because they

could not foresee the modern-day wealth of their applications in numerous areas of science and technology); the other, perhaps more fundamental reason is the nonpropagating nature of the thermal-wave equation. As a pseudowave, the solution set to the thermal-wave Helmholtz equation⁹ is hampered by existence constraints along certain regions of the complex plane defined by the thermal wave vector of the scatterer,¹⁰

$$\tilde{\mathbf{k}}_s = \tilde{k}_\alpha \hat{\mathbf{i}} + \tilde{k}_\beta \hat{\mathbf{j}} + \tilde{k}_\gamma \hat{\mathbf{k}}, \quad (1)$$

where quantities bearing a tilde are complex. The subscript set (α, β, γ) represents general Cauchy contours in the scatterer wave-vector domain, which must be used to define the spatial domain of Green's function for a given geometry.¹⁰ The advantage of the inverse Cauchy contour approach to the thermal-wave Green's function is the associated ability to define explicit, unambiguous ranges of the $\tilde{\mathbf{k}}_s$ complex plane where solutions to the thermal-wave pseudopropagation problem exist and are bounded everywhere within the range. The price paid for this knowledge is the complicated analytical procedure inherent in the requirement for familiarity with complex domain integral manipulations involving nontrivial Cauchy contours with flat segments along the lines $(-\infty e^{\pm i\pi/4}, +\infty e^{\pm i\pi/4})$.¹⁰ All of these complications are intimately associated with the fact that the thermal-wave problem belongs to a class of inverse problems of elliptical type equations known as "ill posed."¹¹

Nevertheless, several authors have successfully used analogies to propagating wave fields to express Green's functions in thermal-wave problems, mainly by *ad hoc* replacing the real wave vector in the Helmholtz equation (or its modifications) by its complex counterpart,^{9,12-14}

$$\tilde{\sigma}(\omega) = (1 + i)(\omega/2\alpha)^{1/2}, \quad (2)$$

where ω is the angular modulation frequency of the thermal wave and α is the thermal diffusivity of the medium in which the thermal wave is excited and pseudopropagates. Owing to the lack of a consistent Green's function formalism with regard to thermal waves, several proposed Green's functions in the literature are incomplete or inconsistent (compare Refs. 9, 12, and 13).

^{a)}Electronic mail: mandelis@me.utoronto.ca

In this article, the equivalence between time t - and frequency-domain thermal diffusion in terms of representations by a Fourier transform pair is exploited to derive internally consistent Cartesian-coordinate thermal-wave Green's functions for infinite, semi-infinite, and finite-size domains in one, two, and three dimensions. Then the thermal-wave fields are expressed in terms of integrals of the derived Green's functions in specific applications to the most common experimental photothermal geometries. This can be called the "thermal-wave Huyghens' Principle," in analogy to conventional wave fields.¹⁵ The present time/frequency Fourier transform pair approach enormously simplifies the derivation of the frequency-domain Green's functions from well-known time-domain representations via a Fourier transformation. The Cauchy contour approach¹⁰ requires the existence of appropriate contours in wave-vector space; that requirement is simply and efficiently transposed here into the requirement for the existence of the Fourier transform of the time-domain Green's function, a far easier task usually assessed by the result of the integration. It is thus hoped that Green's functions obtained in this article will form a mathematically rigorous and useful reference set for experimental and theoretical workers in the field of thermal-wave diagnostics by virtue of the uniqueness, rapidity of convergence/closed-form representations, and globality of Green's functions for all physically acceptable boundary conditions under a fixed geometry. Furthermore, arbitrary source distributions obtained as convolution integrals will be considered, conforming to particular experimental configurations, a powerful generalization of the utility of the present approach.

II. THERMAL-WAVE GREEN'S FUNCTIONS

A. Preliminaries

The starting point is a slight modification of the well-known Green's function for transient diffusion of thermal energy in n dimensions (Ref. 4, Eq. 7.4.10),

$$g(\mathbf{r}-\mathbf{r}_0, t-t_0) = \left(\frac{1}{2\sqrt{\pi\alpha(t-t_0)}} \right)^n \times \exp\left(-\frac{(\mathbf{r}-\mathbf{r}_0)^2}{4\alpha(t-t_0)} \right) H(t-t_0), \quad (3)$$

where \mathbf{r} (\mathbf{r}_0) is the coordinate of the observation (source) point with respect to the origin; t (t_0) is the observation (source appearance) time; and H is the Heavyside function. An impulsive thermal source of unit strength is assumed located at r_0 and acting at the instant t_0 . Equation (3) is the solution to a diffusion equation, the most general (three-dimensional) form of which is

$$\begin{aligned} \nabla^2 g(\mathbf{r}-\mathbf{r}_0, t-t_0) - \frac{1}{\alpha} \frac{\partial}{\partial t} g(\mathbf{r}-\mathbf{r}_0, t-t_0) \\ = -\frac{1}{\alpha} \delta(\mathbf{r}-\mathbf{r}_0) \delta(t-t_0). \end{aligned} \quad (4)$$

It should be noted that the normalization factor ($1/\alpha$) on the right-hand side of Eq. (4) has been inserted so as to yield temperature fields with the right dimensional units. Defining the Fourier transform of Eq. (3) as

$$\tilde{G}(\mathbf{r}-\mathbf{r}_0, t_0; \omega) = \int_{-\infty}^{\infty} g(\mathbf{r}-\mathbf{r}_0, t-t_0) e^{-i\omega t} dt \quad (5)$$

and taking similar Fourier transforms of the various terms in Eq. (4) yields

$$\begin{aligned} \nabla^2 \tilde{G}(\mathbf{r}-\mathbf{r}_0, t_0; \omega) - \frac{i\omega}{\alpha} \tilde{G}(\mathbf{r}-\mathbf{r}_0, t_0; \omega) \\ = -\frac{1}{\alpha} \delta(\mathbf{r}-\mathbf{r}_0) e^{-i\omega t_0}. \end{aligned} \quad (6)$$

Equation (6) can be derived using the boundedness and causality properties of Green's functions,

$$\lim_{t \rightarrow \infty} g(\mathbf{r}-\mathbf{r}_0, t-t_0) = 0 \quad (\text{boundedness}),$$

$$g(\mathbf{r}-\mathbf{r}_0, t-t_0) = 0 \quad \text{for } t < t_0 \quad (\text{causality}).$$

An arbitrary stationary, time-dependent thermal diffusion field generated by a source function $q(\mathbf{r}, t)$ obeys, by analogy to Eq. (4), the following equation:

$$\nabla^2 T(\mathbf{r}, t) - \frac{1}{\alpha} \frac{\partial}{\partial t} T(\mathbf{r}, t) = -\frac{1}{k} q(\mathbf{r}, t), \quad (7)$$

where k is the thermal conductivity of the region containing the source. The Fourier transform of $T(\mathbf{r}, t)$ (assumed existing),

$$\tilde{\theta}(\mathbf{r}, \omega) = \int_{-\infty}^{\infty} T(\mathbf{r}, t) e^{-i\omega t} dt, \quad (8)$$

is the solution to the inhomogeneous thermal-wave equation

$$\nabla^2 \tilde{\theta}(\mathbf{r}, \omega) - \tilde{\sigma}^2(\omega) \tilde{\theta}(\mathbf{r}, \omega) = -\frac{1}{k} \tilde{Q}(\mathbf{r}, \omega), \quad (9)$$

where $\tilde{\sigma}(\omega)$ is given by Eq. (2). $\tilde{Q}(\mathbf{r}, \omega)$ is the Fourier transform of $q(\mathbf{r}, t)$, i.e., the spectrum of the source distribution $q(\mathbf{r}, t)$. Interchanging the coordinates \mathbf{r} and \mathbf{r}_0 in Eq. (6) and replacing \mathbf{r} by \mathbf{r}_0 in Eq. (9) is consistent with the definition of \mathbf{r}_0 as the source coordinate. Then multiplication of Eq. (6) by $\tilde{\theta}(\mathbf{r}_0, \omega)$ and of Eq. (9) by $\tilde{G}(\mathbf{r}_0-\mathbf{r}, t_0; \omega)$, and subtraction and integration over the thermal-wave source volume V_0 yields

$$\begin{aligned} \tilde{\theta}(\mathbf{r}, \omega) e^{-i\omega t_0} = \frac{\alpha}{k} \int \int \int_{V_0} \tilde{Q}(\mathbf{r}_0, \omega) \tilde{G}(\mathbf{r}_0-\mathbf{r}, \omega) dV_0 \\ + \alpha \int \int \int_{V_0} [\tilde{G}(\mathbf{r}_0-\mathbf{r}, \omega) \nabla_0^2 \tilde{\theta}(\mathbf{r}_0, \omega) \\ - \tilde{\theta}(\mathbf{r}_0, \omega) \nabla_0^2 \tilde{G}(\mathbf{r}_0-\mathbf{r}, \omega)] dV_0. \end{aligned} \quad (10)$$

Using the reciprocity property of Green's functions⁴

$$\tilde{G}(\mathbf{r}_0-\mathbf{r}, \omega) = \tilde{G}(\mathbf{r}-\mathbf{r}_0, \omega),$$

and Green's theorem,³ we obtain

$$2\tilde{\theta}(\mathbf{r}, \omega) = \frac{\alpha}{k} \int \int \int_{V_0} \tilde{Q}(\mathbf{r}_0, \omega) \tilde{G}_0(\mathbf{r} - \mathbf{r}_0, \omega) dV_0 + \alpha \oint_{S_0} [\tilde{G}_0(\mathbf{r} - \mathbf{r}_0^s, \omega) \nabla_0 \tilde{\theta}(\mathbf{r}_0^s, \omega) - \tilde{\theta}(\mathbf{r}_0^s, \omega) \nabla_0 \tilde{G}_0(\mathbf{r} - \mathbf{r}_0^s, \omega)] dS_0, \quad (11)$$

$$= \frac{2e^{-i\omega t_0}}{\pi^{3/2} \alpha |\mathbf{r} - \mathbf{r}_0|} \times \int_0^\infty \exp\left(-\xi^2 - \frac{i\omega(\mathbf{r} - \mathbf{r}_0)^2}{4\alpha\xi^2}\right) d\xi, \quad (16)$$

where $\xi^2 = (\mathbf{r} - \mathbf{r}_0)^2 / 4\alpha(t - t_0)$.

Completing the square inside the parentheses of the integrand in Eq. (16) and manipulating finally gives

$$\tilde{G}(\mathbf{r} - \mathbf{r}_0, t_0; \omega) = \frac{2e^{-i\omega t_0}}{\pi^{3/2} \alpha |\mathbf{r} - \mathbf{r}_0|} \exp[-\tilde{\sigma}(\omega)|\mathbf{r} - \mathbf{r}_0|] \times J_1\left(\frac{\tilde{\sigma}(\omega)|\mathbf{r} - \mathbf{r}_0|}{2}\right), \quad (17)$$

where it was defined

$$J_1(A) \equiv \int_0^\infty \exp\left[-\left(x - \frac{A}{x}\right)^2\right] dx. \quad (18)$$

It can be easily shown that, for any A real⁴ or complex, $dJ_1(A)/dA = 0$, i.e., J_1 is independent of A . Setting $A = 0$ gives $J_1(A) = \sqrt{\pi}/2$. Therefore, from Eqs. (17) and (12) the thermal-wave Green's function for an infinite three-dimensional space is

$$\tilde{G}_0(\mathbf{r} - \mathbf{r}_0, \omega) = \frac{e^{\tilde{\sigma}(\omega)|\mathbf{r} - \mathbf{r}_0|}}{\pi\alpha|\mathbf{r} - \mathbf{r}_0|}. \quad (19)$$

This representation is essentially in agreement with earlier forms,^{12,13} except for the constant factor $1/\pi\alpha$ which was replaced with¹² $1/4\pi$ or¹³ $1/4\pi k$, where k is the thermal conductivity of the propagation medium.

C. Three-dimensional semi-infinite Green's function

Two special cases must be considered when a semi-infinite geometry occurs with a dividing surface/interface at the observation coordinate $z=0$, Fig. 1. If the thermal-wave (temperature) field is prescribed at $z=0$, Green's function must satisfy homogeneous Dirichlet boundary conditions in the source coordinate, i.e., at $z_0=0$,

$$\tilde{G}_0(\mathbf{r} - \mathbf{r}_0 | \mathbf{r} - \mathbf{r}'_0, \omega)|_{z_0=0} = 0. \quad (20)$$

As seen in Fig. 1, the coordinate z_0 coincides with the direction normal to the dividing interface. In general, condition (20) must be generalized to involve the normal source coordinate to the tangent plane of any curvilinear coordinate system used. From analogy to the infinite-domain Green's function, an impulsive image source must be placed at \mathbf{r}_0 , such that condition (20) is validated. The appropriate combination is

$$\tilde{G}_0(\mathbf{r} - \mathbf{r}_0 | \mathbf{r} - \mathbf{r}'_0, \omega) = \frac{1}{\pi\alpha} \left(\frac{e^{-\tilde{\sigma}(\omega)|\mathbf{r} - \mathbf{r}_0|}}{|\mathbf{r} - \mathbf{r}_0|} - \frac{e^{-\tilde{\sigma}(\omega)|\mathbf{r} - \mathbf{r}'_0|}}{|\mathbf{r} - \mathbf{r}'_0|} \right). \quad (21)$$

In terms of the coordinate system of Fig. 1

$$|\mathbf{r} - \mathbf{r}_0| = \sqrt{(x - x_0)^2 + (y - y_0)^2 + (z - z_0)^2} \equiv R_0, \quad (22a)$$

where

$$\tilde{G}_0(\mathbf{r} - \mathbf{r}_0, \omega) \equiv \tilde{G}(\mathbf{r} - \mathbf{r}_0, \omega) e^{i\omega t_0} \quad (12)$$

and S_0 is the surface surrounding the source volume V_0 ; \mathbf{r}_0^s is a coordinate point on S_0 . The thermal diffusivity α and conductivity k were assumed to be constant throughout V_0 . A subtle but conceptually important question arises over the existence of the spectrum $\tilde{G}\{\omega\}$ of Green's function $g(\mathbf{r} - \mathbf{r}_0, t - t_0)$, which includes, in principle, all frequencies. Similarly, the "thermal-wave" equation (9) encompasses the entire spectral bandwidth in which the Fourier transform $\tilde{\theta}(\mathbf{r}, \omega)$, Eq. (8), exists. To obtain the conventional thermal-wave behavior¹⁶ the wideband spectral equation (9) must be reduced to a single spectral component form by assuming harmonic thermal excitation at some specific frequency $f_0 = \omega_0/2\pi$. The temperature function can be written from Eq. (8),

$$T(\mathbf{r}, t) = \frac{1}{2\pi} \int_{-\infty}^{\infty} \tilde{\theta}_0(\mathbf{r}, \omega) e^{i\omega t} d\omega = \tilde{\theta}(\mathbf{r}, \omega_0) e^{i\omega_0 t}, \quad (13)$$

where $\tilde{\theta}_0$ is the required thermal-wave kernel function to give the single-frequency component $\tilde{\theta}(\mathbf{r}, \omega_0)$. Inverting Eq. (13) readily yields

$$\tilde{\theta}_0(\mathbf{r}, \omega) = 2\pi \tilde{\theta}(\mathbf{r}, \omega_0) \delta(\omega_0 - \omega). \quad (14)$$

Therefore, once the wideband Fourier spectrum thermal-wave equations (6) and/or (9) have been solved, the single-frequency counterparts can be obtained immediately by replacing ω with ω_0 , or formally

$$\left\{ \begin{array}{l} \tilde{G}_0(\mathbf{r} - \mathbf{r}_0, \omega_0) \\ \tilde{\theta}(\mathbf{r}, \omega_0) e^{i\omega_0 t} \end{array} \right\} = \int_{-\infty}^{\infty} \left\{ \begin{array}{l} \tilde{G}(\mathbf{r} - \mathbf{r}_0, \omega) \\ \tilde{\theta}(\mathbf{r}, \omega) \end{array} \right\} \delta(\omega - \omega_0) e^{i\omega t} d\omega. \quad (15)$$

An important implication concerning the difference between the wideband and single-component versions of \tilde{G} and $\tilde{\theta}$ in Eq. (15) is that, whereas $\tilde{G}(\mathbf{r} - \mathbf{r}_0, \omega)$ and $\tilde{\theta}(\mathbf{r}, \omega)$ may not exist or be ill defined in some regions of the entire spectrum $-\infty < \omega < \infty$, the $\tilde{G}_0(\mathbf{r} - \mathbf{r}_0, \omega_0)$ and $\tilde{\theta}(\mathbf{r}, \omega_0)$ are always assumed to exist and be well defined at ω_0 .

B. Three-dimensional infinite Green's function

Setting $n=3$ in Eq. (3) and using Eq. (5) yields

$$\tilde{G}(\mathbf{r} - \mathbf{r}_0, t_0; \omega) = \frac{1}{2(\pi\alpha)^{3/2}} \int_{t_0}^{\infty} \frac{dt}{(t - t_0)^{3/2}} \times \exp\left(-\frac{(\mathbf{r} - \mathbf{r}_0)^2}{4\alpha(t - t_0)} - i\omega t\right)$$

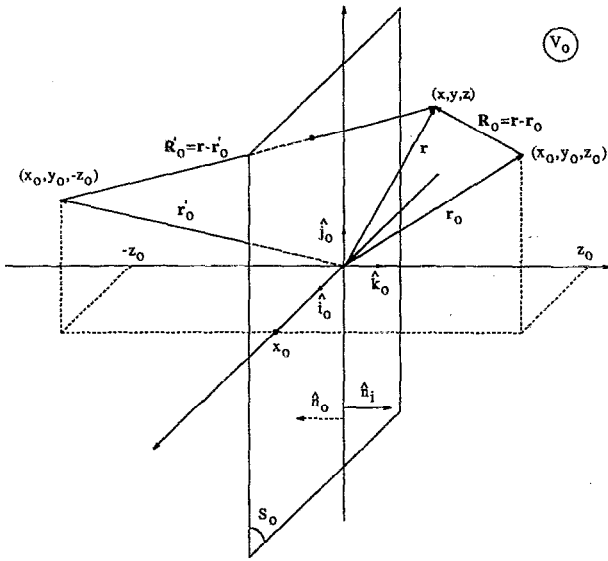


FIG. 1. Coordinate system for three-dimensional (x_0, y_0, z_0) geometry with $z_0=0$ plane (S_0) separating two half-spaces. (x, y, z) : observation coordinates; (x_0, y_0, z_0) : source coordinates. $R_0 = |\mathbf{R}_0| = |\mathbf{r} - \mathbf{r}_0| = \sqrt{(x-x_0)^2 + (y-y_0)^2 + (z-z_0)^2}$; $R'_0 = |\mathbf{R}'_0| = |\mathbf{r} - \mathbf{r}'_0| = \sqrt{(x-x_0)^2 + (y-y_0)^2 + (z+z_0)^2}$; $\hat{\mathbf{n}}_0$: unit outward vector to volume V_0 ; $\hat{\mathbf{n}}_i$: unit inward vector to volume V_0 .

$$|\mathbf{r} - \mathbf{r}'_0| = \sqrt{(x-x_0)^2 + (y-y_0)^2 + (z+z_0)^2} \equiv R'_0. \quad (22b)$$

At $z_0=0$ we obtain

$$|\mathbf{r} - \mathbf{r}_0| = |\mathbf{r} - \mathbf{r}'_0| = \sqrt{(x-x_0)^2 + (y-y_0)^2 + z^2} \equiv R. \quad (23)$$

Equation (21) is similar to a generalization of the infinite domain Green's function derived independently⁹ using a thermal-wave diffraction integral formalism, with the exception of the exponential terms which in that treatment appear as $e^{i\tilde{\sigma}|r-r_0|}$ and $e^{i\tilde{\sigma}|r-r'_0|}$. The cause of this apparent discrepancy is the choice of the sign of the Fourier component of the temperature field as $e^{i\omega t}$ in the framework of Eq. (8). This choice renders positive the sign of the θ -dependent term in Eq. (9). Overall this remark is meant to emphasize the importance of sign conventions in thermal-wave physics as a possible source of error, unlike in the conventional Helmholtz equations obtained with propagating wave fields, where the sign of the time-harmonic term $e^{\pm i\omega t}$ is immaterial due to the second time derivatives from which the Helmholtz equations are derived.

If the thermal-wave flux is prescribed at the interface $z=0$, Green's function must satisfy homogeneous Neumann boundary conditions in the source coordinate at $z=0$,

$$\nabla_0 \tilde{G}_0(\mathbf{r} - \mathbf{r}_0 | \mathbf{r} - \mathbf{r}'_0, \omega) |_{z_0=0} = 0. \quad (24)$$

∇_0 indicates the normal derivative of \tilde{G}_0 along the normal source coordinates z_0 at the interface. The impulsive image source argument applies here with the requirement that the thermal-wave fluxes cancel out at the interface. The appropriate combination is

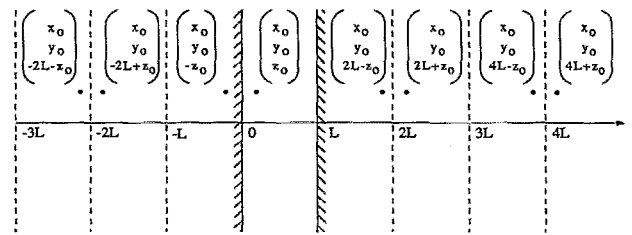


FIG. 2. Image source locations in three-dimensional application of the method of images to thermal-wave Green's function formulation.

$$\tilde{G}_0(\mathbf{r} - \mathbf{r}_0 | \mathbf{r} - \mathbf{r}'_0, \omega)$$

$$= \frac{1}{\pi\alpha} \left(\frac{e^{-\tilde{\sigma}(\omega)|r-r_0|}}{|r-r_0|} + \frac{e^{-\tilde{\sigma}(\omega)|r-r'_0|}}{|r-r'_0|} \right), \quad (25)$$

corresponding to the situation shown in Fig. 1. A different version of Green's function Eq. (25) has been previously presented independently,¹³ but without derivation. The main differences appear in the exponents in the form $e^{i\tilde{\sigma}|r-r_0|}$ and $e^{i\tilde{\sigma}|r-r'_0|}$ and, in view of the earlier discussion, they are likely to be traced in the sign of the time-harmonic term $e^{\pm i\omega t}$.

D. Three-dimensional Green's function for finite geometries: Method of images

The method of images is well suited for situations where Green's function is known for an infinite geometry and it is required for a geometry with finite boundaries. In that case the infinite-geometry function may be used as a basis, extended by inclusion of a multiple infinity of source terms, each infinite sum representing "reflections" with respect to a particular boundary in order to satisfy prescribed boundary conditions. In that sense, the foregoing three-dimensional semi-infinite Green's function Eq. (25) can be viewed as the result of the application of the method of images at the interface which defines the semi-infinite geometry. Historically Thomas *et al.*^{12,13} and Mandelis and Power¹⁷ have presented analytical solutions to thermal-wave problems involving angled or flat boundaries of finite dimensions using the method of images. The results of the method of images to be presented below are mathematically strictly valid and yield correct Green's functions which can also be derived independently from the governing differential equation.

Based on the mathematical convenience of the method of images, the infinite-domain Green's function Eq. (19) can be extended to accommodate plane bounding surfaces at $z=0, L$ with infinite radial dimensions. In a manner similar to the derivation of Eq. (21) for semi-infinite domains, image sources must be placed at source coordinates as shown in Fig. 2, so as to satisfy either Dirichlet or Neumann boundary conditions at $z=0, L$. The resulting Green's functions are

$$\tilde{G}_0(\mathbf{r} - \mathbf{r}_0 | \mathbf{r} - \mathbf{r}'_0, \omega) = \frac{1}{\pi\alpha} \sum_{n=-\infty}^{\infty} \left(\frac{e^{-\tilde{\sigma}(\omega)|r-r_{0n}|}}{|r-r_{0n}|} \mp \frac{e^{-\tilde{\sigma}(\omega)|r-r'_{0n}|}}{|r-r'_{0n}|} \right), \quad (26)$$

where (\mp) corresponds to Dirichlet/Neumann boundary conditions and, upon combination of the coordinate system of Fig. 1 with the array of image sources of Fig. 2,

$$|\mathbf{r}-\mathbf{r}_{0n}|=\sqrt{(x-x_0)^2+(y-y_0)^2+[z-(2nL+z_0)]^2} \quad (27a)$$

and

$$|\mathbf{r}-\mathbf{r}'_{0n}|=\sqrt{(x-x_0)^2+(y-y_0)^2+[z-(2nL-z_0)]^2}. \quad (27b)$$

E. Two-dimensional Green's functions

Setting $n=2$ in Eq. (3) and inserting in Eq. (5) gives

$$\begin{aligned} \tilde{G}(\mathbf{r}-\mathbf{r}_0, t_0; \omega) \\ = \frac{1}{4\pi\alpha} \int_{t_0}^{\infty} \frac{dt}{t-t_0} \exp\left(-\frac{(\mathbf{r}-\mathbf{r}_0)^2}{4\alpha(t-t_0)} - i\omega t\right). \end{aligned} \quad (28)$$

Using a change of variable similar to Eq. (16) results in the following representation:

$$\tilde{G}_0(\mathbf{r}-\mathbf{r}_0, \omega) = \frac{1}{2\pi\alpha} \int_0^{\infty} \frac{d\xi}{\xi} \exp\left[-\left(\xi^2 + \frac{i\omega(\mathbf{r}-\mathbf{r}_0)^2}{4\alpha\xi^2}\right)\right]. \quad (29)$$

This integral has been tabulated (Ref. 18, entry 3.478.4) and yields

$$\tilde{G}_0(\mathbf{r}-\mathbf{r}_0, \omega) = \frac{1}{2\pi\alpha} K_0[\tilde{\sigma}(\omega)|\mathbf{r}-\mathbf{r}_0|], \quad (30)$$

where K_0 is the Kelvin function of order zero. This Green's function has been derived independently¹⁰ using a complex Cauchy contour and it has been shown¹⁰ that the integration path of its integral representation is different from the one conventionally used in the treatment of Bessel functions of complex argument,¹⁹ owing to the rotated Cauchy contour in thermal wave-vector space. In practice, the real and imaginary parts of Green's function Eq. (30) may be separated out easily for computations in terms of Thomson functions,¹⁹

$$\begin{aligned} \tilde{G}_0(\mathbf{r}-\mathbf{r}_0, \omega) = \frac{1}{2\pi\alpha} \left\{ \ker\left[\left(\frac{\omega}{\alpha}\right)^{1/2} |\mathbf{r}-\mathbf{r}_0|\right] \right. \\ \left. + i \operatorname{kei}\left[\left(\frac{\omega}{\alpha}\right)^{1/2} |\mathbf{r}-\mathbf{r}_0|\right] \right\}. \end{aligned} \quad (31)$$

Series expansions and asymptotic representations for the Thomson functions can be found in Ref. 18, entries 8.564 and 8.566. Green's function (30) has been used in the generation of computational algorithms for thermal-wave slice diffraction tomography (TSDT).^{20,21} A problem with the two-dimensional thermal-wave Green's function is the strong singularity encountered at the origin, which makes it difficult to use for field descriptions in the neighborhood of point sources commonly occurring with highly focused laser heating. The strong singularity at the origin is not particular to the thermal-wave field, but is endemic to two-dimensional Green's functions describing steady waves.⁴ For this reason, it is computationally preferable to use three-dimensional forms of Green's function along a fixed coordinate to describe two-dimensional thermal-wave fields. Therefore, the development of two-dimensional expressions for bounded geometries, albeit central to the TSDT problem^{20,21} and to

applications of photothermal beam deflection methods,^{22,23} will not be pursued further here. It can be easily approached in a straightforward manner by use of extensions of Eq. (30) in combination with the method of images.

F. One-dimensional Green's functions

Setting $n=1$ in Eq. (3) and following the same procedure yields for the infinite-domain Green's function

$$\begin{aligned} G(x-x_0, t_0; \omega) = \frac{1}{2\sqrt{\pi\alpha}} \int_{t_0}^{\infty} \frac{dt}{(t-t_0)^{1/2}} \\ \times \exp\left(-\frac{(x-x_0)^2}{4\alpha(t-t_0)} - i\omega t\right), \end{aligned} \quad (32)$$

where the spatial coordinate was assumed to be along the x axis. Transformation of the variable to $\xi^2=(x-x_0)^2/4\alpha(t-t_0)$ gives

$$\tilde{G}_0(x-x_0, \omega) = \frac{|x-x_0|}{2\sqrt{\pi\alpha}} e^{-\tilde{\sigma}(\omega)|x-x_0|} J_2\left(\frac{\tilde{\sigma}(\omega)|x-x_0|}{2}\right), \quad (33)$$

where it was defined that

$$J_2(A) \equiv \int_0^{\infty} \frac{dx}{x^2} \exp\left[-\left(x - \frac{A}{x}\right)^2\right]. \quad (34)$$

It can be easily shown by the change of variable $y=A/x$ that

$$\frac{dJ_2(A)}{dA} = -\frac{1}{A^2} J_1(A), \quad (35)$$

where $J_1(A)$ is given by Eq. (18) and has the value⁴ $J_1(A) = \sqrt{\pi}/2$. Therefore, $J_2(A) = \sqrt{\pi}/2A$ and Green's function becomes

$$\tilde{G}_0(x-x_0, \omega) = \frac{1-i}{2\sqrt{2\alpha\omega}} e^{-\tilde{\sigma}(\omega)|x-x_0|}. \quad (36)$$

It follows that the semi-infinite domain Green's function is

$$\begin{aligned} \tilde{G}_0(x-x_0|x+x_0, \omega) \\ = \frac{1-i}{2\sqrt{2\alpha\omega}} (e^{-\tilde{\sigma}(\omega)|x-x_0|} \mp e^{-\tilde{\sigma}(\omega)(x+x_0)}), \end{aligned} \quad (37)$$

where the use of \mp signifies that the function satisfies the Dirichlet/Neumann boundary conditions. Finally, direct application of the method of images, Fig. 2, gives Green's function for a thin rod of material bounded by $x=0, L$,

$$\begin{aligned} \tilde{G}_0(x|x_0, \omega) = \frac{1-i}{2\sqrt{2\alpha\omega}} \sum_{n=-\infty}^{\infty} (e^{-\tilde{\sigma}(\omega)|x-(2nL+x_0)|} \\ \mp e^{-\tilde{\sigma}(\omega)|x-(2nL-x_0)|}). \end{aligned} \quad (38)$$

III. SOME APPLICATIONS OF GREEN'S FUNCTIONS

A. One-dimensional thermal-wave fields

1. Case I: A semi-infinite rod with temperature at $x=0$ given by $\theta(0, t) = T_0 e^{i\omega_0 t}$

This problem has been previously treated⁴ using the time-domain Green's function, Eq. (3) with $n=1$. The

thermal-wave Green's function must satisfy a homogeneous Dirichlet condition at the source coordinate $x_0=0$. From Eq. (11) in one dimension, with $Q(x_0, \omega)=0$ (no bulk/volume sources), and Eq. (37) with $\tilde{G}_0(x-x_0, \omega)=0$ (homogeneous Dirichlet boundary condition), we obtain

$$\tilde{\theta}(x, \omega) = -\alpha \tilde{\theta}(x_0=0, \omega) [\nabla_0 \tilde{G}_0(x-x_0, \omega)|_{x_0=0}] \cdot \hat{\mathbf{n}}_i, \quad (39)$$

where the boundary surface integral over S_0 has degenerated to a single point $x_0=0$ and the vector normal to the surface dS_0 has been replaced by $\hat{\mathbf{n}}_i$ the inward unit vector parallel to the z axis indicating the in-flow of thermal energy. In the same spirit we define

$$\nabla_0 = \hat{\mathbf{n}}_0 \frac{\partial}{\partial x_0} = -\hat{\mathbf{n}}_i \frac{\partial}{\partial x_0}, \quad (40)$$

where $\hat{\mathbf{n}}_0$ is the outward unit vector. Therefore, Eq. (39) becomes

$$\tilde{\theta}(x, \omega) = \alpha \theta(0, t) \left(\frac{\partial}{\partial x_0} \tilde{G}_0(x-x_0, \omega) \Big|_{x_0=0} \right), \quad (41)$$

and from Eq. (37),

$$\begin{aligned} \frac{\partial}{\partial x_0} \tilde{G}_0(x-x_0, \omega) \\ = \frac{(1-i)\tilde{\sigma}(\omega)}{2\sqrt{2\alpha\omega}} (e^{-\tilde{\sigma}(\omega)(x-x_0)} + e^{-\tilde{\sigma}(\omega)(x+x_0)}), \end{aligned} \quad (42)$$

where the $|x-x_0|$ was replaced by $(x-x_0)$, because $x > x_0^s = 0$ for all observation coordinates $x > 0$ along the semi-infinite rod. For the same reason, in evaluating $\partial \tilde{G}_0 / \partial x_0$ we must set $d|x-x_0|/dx_0 = -1$. Collecting terms,

$$\tilde{\theta}(x, \omega) = \theta(0, t) e^{-\tilde{\sigma}(\omega)x} = T_0 e^{i\omega_0 t - \tilde{\sigma}(\omega)x}. \quad (43)$$

It should be recalled that $\tilde{\theta}(x, \omega)$ is the wideband Fourier spectrum of the required thermal-wave field.

Finally, using the transformation indicated by Eqs. (13) and (14) yields

$$T(x, t) = T_0 e^{i\omega_0 t - \tilde{\sigma}(\omega_0)x} \equiv T(x, \omega_0). \quad (44)$$

This equation represents the semi-infinite one-dimensional thermal-wave field and is identical to Morse and Feshbach's Eq. (7.4.14).⁴

2. Case II: The same semi-infinite rod with prescribed thermal-wave surface flux at $x=0$ given by $\phi(0, t) = \phi_0 e^{i\omega_0 t}$

Green's function must satisfy a homogeneous Neumann condition at the source coordinate $x_0=0$, i.e.,

$$\frac{\partial}{\partial x_0} \tilde{G}_0(x-x_0, \omega) \Big|_{x_0=0} = 0. \quad (45)$$

Therefore, Eq. (11) in the absence of bulk sources becomes

$$\tilde{\theta}(x, \omega) = \alpha [\tilde{G}_0(x-x_0, \omega) \Big|_{x_0=0}] [\nabla_0 \tilde{\theta}(x_0, \omega) \Big|_{x_0=0}] \cdot \hat{\mathbf{n}}_i \quad (46a)$$

$$= -\frac{(1-i)\alpha}{2\sqrt{2\alpha\omega}} (2e^{-\tilde{\sigma}(\omega)x}) \frac{\partial}{\partial x_0} \tilde{\theta}(x_0, \omega) \Big|_{x_0=0}. \quad (46b)$$

In deriving Eq. (46) the same $\hat{\mathbf{n}}$ and ∇_0 conventions used in Case I were applied. To evaluate the $\partial \tilde{\theta} / \partial x_0$ at $x_0=0$, the incident flux $\phi(0, t)$ must be introduced in the source coordinate x_0 . From the definition of thermal flux one obtains

$$\frac{\partial}{\partial x_0} \tilde{\theta}(x_0, \omega) \Big|_{x_0=0} = -\left(\frac{\phi_0}{k} \right) e^{i\omega_0 t}, \quad (47)$$

where k is the thermal conductivity of the rod.

Therefore, Eqs. (46) and (47) yield the thermal-wave spectrum

$$\tilde{\theta}(x, \omega) = \frac{(1-i)\sqrt{\alpha}\phi_0}{k\sqrt{2\omega}} e^{-\tilde{\sigma}(\omega)x + i\omega_0 t} \quad (48)$$

or, upon inversion,

$$T(x, t) = \phi_0 \left(\frac{\sqrt{\alpha}}{k} \right) \frac{1}{\sqrt{\omega_0}} e^{i\omega_0 t - [\tilde{\sigma}(\omega_0)x + (i\pi/4)]} \equiv T(x, \omega_0). \quad (49)$$

The resulting thermal-wave field $T(x, \omega_0)$ exhibits the well-known $\pi/4$ phase lag with respect to the input thermal-wave flux predicted for semi-infinite geometries (Ref. 5(a), Chap. 2.6).

3. Case III: The thermal-wave problem of case II for a thin rod of length L and flux $\phi(0, t)$ at $x=0$

Green's function must satisfy homogeneous Neumann conditions at $x=0, L$. Owing to the finite length of the rod, the appropriate Green's function is given by Eq. (38) (+ sign). For convenience the summation can be split up into two components $0 \leq n < \infty$, $-1 \geq n > -\infty$ and redefined,

$$\begin{aligned} \tilde{G}_0(x|x_0, \omega) = \frac{1-i}{2\sqrt{2\alpha\omega}} \left(e^{-\tilde{\sigma}(\omega)|x-x_0|} + e^{-\tilde{\sigma}(\omega)(x+x_0)} \right. \\ \left. + \sum_{n=1}^{\infty} (e^{-\tilde{\sigma}(\omega)|x-(2nL+x_0)|} \right. \\ \left. + e^{-\tilde{\sigma}(\omega)|x-(2nL-x_0)|} + e^{-\tilde{\sigma}(\omega)|x+2nL-x_0|} \right. \\ \left. + e^{-\tilde{\sigma}(\omega)(x+2nL+x_0)} \right). \end{aligned} \quad (50)$$

The thermal-wave spectrum is given by Eq. (46a), although formally a similar term evaluated at $x_0=L$ must be added to account for the "other side" of the bounding surface S_0 . However, $\nabla_0 \tilde{\theta}(x_0, \omega) \Big|_{x_0=L} = 0$, because incident flux occurs only at $x_0=0$. Using Green's function Eq. (50) and Eqs. (47) and (46a) yields

$$\begin{aligned} \tilde{\theta}(x, \omega) = \frac{(1-i)\sqrt{\alpha}}{k\sqrt{2\omega}} \phi_0 e^{i\omega_0 t} \left(e^{-\tilde{\sigma}(\omega)x} + \sum_{n=1}^{\infty} (e^{-\tilde{\sigma}(\omega)(2nL-x)} \right. \\ \left. + e^{-\tilde{\sigma}(\omega)(2nL+x)}) \right). \end{aligned} \quad (51)$$

Performing the infinite summations and inverting the resulting thermal-wave spectrum finally gives

$$T(x, \omega_0) = \phi_0 \left(\frac{\sqrt{\alpha}}{k} \right) \frac{1}{\sqrt{\omega_0}} \left(\frac{e^{-\tilde{\sigma}(\omega_0)x} + e^{-\tilde{\sigma}(\omega_0)(2L-x)}}{1 - e^{-2\tilde{\sigma}(\omega_0)L}} \right) \times e^{i[\omega_0 t - (\pi/4)]} \quad (52)$$

This equation readily simplifies to Eq. (49) in the limit $L \rightarrow \infty$, as expected. It is familiar from other solution methodologies, usually by direct solution of the thermal-wave equation,²⁴ Eq. (9), for applications in backscattered ($x=0$) or transmission ($x=L$) photothermal diagnostics.

B. Three-dimensional thermal-wave fields

1. Case I: A semi-infinite (half-space) region with thermal-wave flux prescribed over the interface plane $z_0=0$

In this case,

$$\phi(\mathbf{r}_s, t) = \phi_0 e^{-r_s^2/w^2} e^{i\omega_0 t}, \quad (53)$$

generated by a Gaussian laser beam of spot size w . In this case Green's function must satisfy a homogeneous Neumann boundary condition on the source plane $z_0=0$ and is given by Eq. (25). It is further assumed that no volume sources exist in the half-space (x_0, y_0, z_0) where the thermal-wave field is sought, Fig. 3. Therefore, the solution Eq. (11) becomes

$$\tilde{\theta}(\mathbf{r}, \omega) = \alpha \iint_{S_0} \tilde{G}_0(\mathbf{r} - \mathbf{r}_0^S | \mathbf{r} - \mathbf{r}_0^S, \omega) \nabla_0 \tilde{\theta}(\mathbf{r}_0^S, \omega) \cdot d\mathbf{S}_0, \quad (54)$$

where $d\mathbf{S}_0$ must be replaced by $d\mathbf{S}_i = \hat{\mathbf{n}}_i dx_0 dy_0$ pointing in the direction inside the half-space V_0 to indicate in-flow of thermal energy. The surface S_0 is the plane $z_0=0$. Furthermore,

$$\nabla_0 = \hat{\mathbf{n}}_0 \frac{\partial}{\partial z_0} = -\hat{\mathbf{n}}_i \frac{\partial}{\partial z_0}, \quad (55)$$

so that from the definition of thermal flux

$$\begin{aligned} \phi(\mathbf{r}_s, t) &= \phi(x_0, y_0, 0; t) = -k \frac{\partial}{\partial z_0} \tilde{\theta}(x_0, y_0, z_0; t) \Big|_{z_0=0} \\ &= \phi_0 e^{i\omega_0 t} \exp\left(-\frac{(x_0^2 + y_0^2)}{w^2}\right), \end{aligned} \quad (56)$$

or

$$\nabla_0 \tilde{\theta}(\mathbf{r}_0^S, \omega) = \hat{\mathbf{n}}_i \left(\frac{\phi_0}{k} \right) e^{i\omega_0 t} \exp\left(-\frac{(x_0^2 + y_0^2)}{w^2}\right). \quad (57)$$

Equations (25), (54), and (57) give the spectrum of the thermal-wave field in form of an integral over the bounding interface $S_0(x_0, y_0)$;

$$\begin{aligned} \tilde{\theta}(\mathbf{r}, \omega) &= \frac{2\phi_0}{\pi k} e^{i\omega_0 t} \int \int_{-\infty}^{\infty} \frac{dx_0 dy_0}{R} \\ &\times \exp\left(-\frac{(x_0^2 + y_0^2)}{w^2} - \tilde{\sigma}(\omega)R\right), \end{aligned} \quad (58)$$

where R was defined in Eq. (23). A change of variables $x - x_0 = \eta$ and $y - y_0 = \xi$ recasts Eq. (58) in the form

$$\tilde{\theta}(\mathbf{r}, \omega) = \frac{2\phi_0}{\pi k} e^{i\omega_0 t} \exp\left(-\frac{(x^2 + y^2)}{w^2}\right) J_3(x, y, z), \quad (59)$$

with

$$\begin{aligned} \tilde{J}_3(x, y, z) &\equiv \iint_{-\infty}^{\infty} \frac{d\eta d\xi}{\sqrt{\eta^2 + \xi^2 + z^2}} \\ &\times \exp\left(-\tilde{\sigma}(\omega) \sqrt{\eta^2 + \xi^2 + z^2} - \frac{[\eta^2 + \xi^2 - 2(\eta x + \xi y)]}{w^2}\right). \end{aligned} \quad (60)$$

A final variable change to $\rho^2 = \eta^2 + \xi^2$ can separate out the two components of the surface integral, so that

$$\begin{aligned} \tilde{J}_3(x, y, z) &= \int_0^{\infty} \frac{\rho d\rho}{\sqrt{\rho^2 + z^2}} \exp\left(-\tilde{\sigma}(\omega) \sqrt{\rho^2 + z^2} - \frac{\rho^2}{w^2}\right) \\ &\times \int_0^{2\pi} d\theta e^{2\rho(x \cos \theta + y \sin \theta)/w^2}. \end{aligned} \quad (61)$$

The angular integral can be readily evaluated from (Ref. 18, entry 3.937.2, p. 488)

$$\int_0^{2\pi} e^{p \cos x + q \sin x} dx = 2\pi I_0(\sqrt{p^2 + q^2}), \quad (62)$$

where I_0 is the modified Bessel function of order zero. The resulting integral is

$$\begin{aligned} \tilde{J}_3(x, y, z) &= 2\pi \int_0^{\infty} \frac{\rho d\rho}{\sqrt{\rho^2 + z^2}} \exp\left(-\frac{\rho^2}{w^2} - \tilde{\sigma}(\omega) \sqrt{\rho^2 + z^2}\right) \\ &\times I_0\left(\frac{2\rho}{w^2} \sqrt{x^2 + y^2}\right). \end{aligned} \quad (63)$$

The thermal-wave field represented by Eqs. (59) and (63) is in a compact form which can be easily evaluated numerically using the polynomial approximation for $I_0(x)$ given in Ref. 25, entries 9.8.1–9.8.4. The relatively simple expression for the spectrum $\tilde{\theta}(\mathbf{r}, \omega)$ and, by extension, for the thermal-wave field $T(\mathbf{r}, t) \equiv T(x, y, z; \omega_0)$ is in the form of a single integral by virtue of Green's function analysis. This approach should be compared with the complexity of the eigenfunction ex-

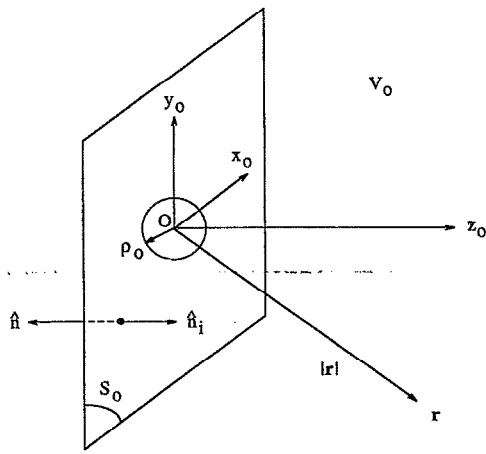


FIG. 3. Geometry for calculation of semi-infinite thermal-wave field generated by a Gaussian laser beam totally absorbed at the surface plane $z_0=0$.

pansion solution to the thermal-wave differential equation (9) in terms of infinite series which is frequently of slow convergence.²⁶ It should also be compared with thermal-wave (photoacoustic) Green's function formulations based on infinite series of eigenfunction expansions,¹⁴ where also series complexity and speed of convergence can be primary disadvantages. It is the enormous advantage of the elegance and numerical simplicity of single integrals such as J_3 in Eq. (63) that ultimately justifies the use of integral Green's function analysis in problems of higher dimensions than one.

2. Case II: The thermal-wave problem of case I, bounded by plane interfaces at $z_0=0, L$

In a manner similar to case I, and in the absence of bulk (volume) sources, the field equation is given by Eq. (54) where S_0 encompasses only the plane $z_0=0$, because at $z_0=L$ the thermal-wave flux is zero (no source). The relevant Green's function now is Eq. (26) satisfying homogeneous Neumann conditions at the two interface planes. Equation (54) gives

$$\begin{aligned} \bar{\theta}(\mathbf{r}, \omega) = & -\frac{1}{\pi} \left(\frac{\partial}{\partial z_0} \bar{\theta}(x_0, y_0, z_0; \omega_0) \Big|_{z_0=0} \right) \\ & \times \sum_{n=-\infty}^{\infty} \left(\frac{e^{-\bar{\sigma}(\omega)|\mathbf{r}-\mathbf{r}_{0n}|}}{|\mathbf{r}-\mathbf{r}_{0n}|} + \frac{e^{-\bar{\sigma}(\omega)|\mathbf{r}-\mathbf{r}'_{0n}|}}{|\mathbf{r}-\mathbf{r}'_{0n}|} \right)_{z_0=0}, \end{aligned} \quad (64)$$

where $\partial\bar{\theta}/\partial z_0$ is given by Eq. (56). Now defining integrals

$$\begin{aligned} \tilde{J}_4^{(n)}(x, y; A_n) \equiv & 2\pi \int_0^\infty \frac{\rho d\rho}{\sqrt{\rho^2 + A_n^2}} \exp\left(-\frac{\rho^2}{w^2}\right) \\ & - \bar{\sigma}(\omega) \sqrt{\rho^2 + A_n^2} I_0\left(\frac{2\rho}{w^2} \sqrt{x^2 + y^2}\right) \end{aligned} \quad (65)$$

and splitting up the summation in Eq. (64) results in the expression

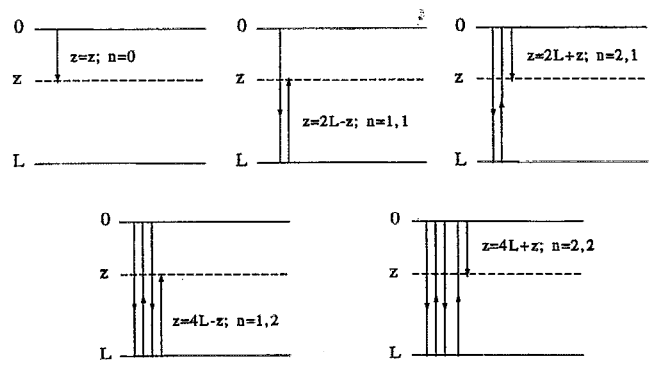


FIG. 4. Buildup of thermal-wave field at an arbitrary depth z inside a region bounded by plane interfaces $z=0, L$, by use of mathematically convenient thermal ray "reflection" and superposition.

$$\begin{aligned} \bar{\theta}(\mathbf{r}, \omega) = & \frac{2\phi_0}{\pi k} e^{i\omega_0 t} \exp\left(-\frac{(x^2 + y^2)}{w^2}\right) \left(\tilde{J}_3(x, y, z) \right. \\ & \left. + \sum_{n=1}^{\infty} [\tilde{J}_4^{(n)}(x, y; 2nL - z) + \tilde{J}_4^{(n)}(x, y; 2nL + z)] \right) \end{aligned} \quad (66)$$

for the thermal-wave field spectrum. The backscattered thermal-wave field Eq. (13) becomes

$$\begin{aligned} T(x, y, 0; \omega_0) = & \frac{2\phi_0}{\pi k} e^{i\omega_0 t} \exp\left(-\frac{(x^2 + y^2)}{w^2}\right) \left(\tilde{J}_3(x, y, 0) \right. \\ & \left. + 2 \sum_{n=1}^{\infty} \tilde{J}_4^{(n)}(x, y; 2nL) \right) \end{aligned} \quad (67a)$$

and the transmitted thermal wave field is

$$\begin{aligned} T(x, y, L; \omega_0) = & \frac{2\phi_0}{\pi k} e^{i\omega_0 t} \exp\left(-\frac{(x^2 + y^2)}{w^2}\right) \\ & \times \left(\tilde{J}_3(x, y, L) + \sum_{n=1}^{\infty} \{ \tilde{J}_4^{(n)}[x, y; (2n+1)L] \right. \\ & \left. + \tilde{J}_4^{(n)}[x, y; (2n-1)L] \} \right). \end{aligned} \quad (67b)$$

These three-dimensional field summations cannot be represented by compact formulas such as Eq. (52) for the one-dimensional geometry of finite thickness. A convenient mathematical (but physically heuristic) interpretation is that of Fig. 4 in terms of infinite "reflections" of thermal "rays" at the interfaces $z=0, L$. In Fig. 4 the double index $n:(i, j)$ corresponds to specific terms (i) and (j) of the first summation $\sum_{i=1}^{\infty} \tilde{J}_4^{(i)}(x, y; 2iL - z)$ and of the second summation $\sum_{j=1}^{\infty} \tilde{J}_4^{(j)}(x, y; 2jL + z)$, respectively, in Eq. (66).

IV. CONCLUSIONS

Consistent Green's function representations of homogeneous thermal-wave fields were formulated for one, two, and three spatial dimensions in Cartesian coordinates and infinite, semi-infinite, and bounded geometries. The formalisms were based on integral equations for the thermal-wave fields and some applications were presented in one and three dimensions. Two-dimensional cases can be easily treated using the three-dimensional analysis with one spatial coordinate fixed. Several inconsistencies of Green's functions published in the thermal-wave literature were thus addressed and new integral formulas suitable for computer implementation featuring rapid convergence (tested in this laboratory) in the case of three-dimensional fields generated by laser photo-thermal excitation were derived. It is hoped that the foregoing treatment will stimulate the use of Green's function approaches to various thermal-wave problems by future investigators who wish to take advantage of their elegance, simplicity, and general power in closed-form (albeit as an integral) description of diverse geometries under arbitrary boundary conditions. Extensions of the present Green's functions derivations in curvilinear coordinate systems are under consideration.

ACKNOWLEDGMENTS

The support of the Natural Sciences and Engineering Research Council of Canada and of the Manufacturing Research Corporation of Ontario is gratefully acknowledged.

¹ *Principles and Perspectives of Photothermal and Photoacoustic Phenomena*, Progress in Photothermal and Photoacoustic Science and Technology, Vol. 1, edited by A. Mandelis (North-Holland, New York, 1991).

² *Non-Destructive Evaluation*, Progress in Photothermal and Photoacoustic Science and Technology, Vol. 2, edited by A. Mandelis (PTR Prentice Hall, Englewood Cliffs, NJ, 1993).

- ³ E. Kreyszig, *Advanced Engineering Mathematics*, 7th ed. (Wiley, New York, 1993), Chap. 9.
- ⁴ P. M. Morse and H. Feshbach, *Methods of Theoretical Physics* (McGraw-Hill, New York, 1953), Chap. 7.4.
- ⁵ (a) H. S. Carslaw and J. C. Jaeger, *Conduction of Heat in Solids*, 2nd ed. (Clarendon, Oxford, 1959), Chap. 14; (b) M. N. Ozisik, *Boundary Value Problems of Heat Conduction* (Dover, New York, 1968), Chap. 5.
- ⁶ A. Rose, R. Vyas, and R. Gupta, *Appl. Opt.* **25**, 4626 (1984).
- ⁷ A. Mandelis, in *Photoacoustic, Photothermal and Photochemical Processes at Surfaces and in Thin Films*, Topics in Current Physics, Vol. 47, edited by P. Hess (Springer, Heidelberg, 1989), p. 211.
- ⁸ V. S. Arpaci, *Conduction Heat Transfer* (Addison-Wesley, Reading, MA, 1966), Chap. 6.
- ⁹ A. Mandelis, *J. Opt. Soc. Am. A* **6**, 298 (1989).
- ¹⁰ A. Mandelis, *J. Phys. A* **24**, 2485 (1991).
- ¹¹ V. B. Glasko, *Inverse Problems of Mathematical Physics* (Am. Inst. Phys., New York, 1984).
- ¹² R. L. Thomas, J. J. Pouch, Y. H. Wong, L. D. Favro, P.-K. Kuo, and A. Rosencwaig, *J. Appl. Phys.* **51**, 1152 (1980).
- ¹³ L. D. Favro, P.-K. Kuo, and R. L. Thomas, in *Photoacoustic and Thermal Wave Phenomena in Semiconductors*, edited by A. Mandelis (North-Holland, New York, 1987), Chap. 4.
- ¹⁴ H. C. Chow, *J. Appl. Phys.* **51**, 4053 (1980).
- ¹⁵ K. J. Langenberg, *Applied Inverse Problems* (Fraunhofer Institut für Zerstörungsfreie Prüfverfahren, Kassel, 1986).
- ¹⁶ A. Rosencwaig and A. Gersho, *J. Appl. Phys.* **47**, 64 (1976).
- ¹⁷ A. Mandelis and J. F. Power, *Appl. Opt.* **27**, 3397 (1988).
- ¹⁸ I. S. Gradshteyn and I. M. Ryzhik, *Table of Integrals, Series and Products*, English translation, edited by A. Jeffrey (Academic, Orlando, 1980).
- ¹⁹ G. N. Watson, *A Treatise on the Theory of Bessel Functions*, 2nd ed. (Cambridge University Press, Cambridge, 1958).
- ²⁰ O. Padé and A. Mandelis, *Rev. Sci. Instrum.* **64**, 3548 (1993).
- ²¹ O. Padé and A. Mandelis, *Inverse Problems* **10**, 185 (1994).
- ²² P.-K. Kuo, L. J. Inglehart, E. D. Sendler, M. J. Lin, L. D. Favro, and R. L. Thomas, *Rev. Prog. Non-Destruct. Eval.* **4B**, 745 (1985).
- ²³ P.-K. Kuo, E. D. Sendler, L. D. Favro, and R. L. Thomas, *Can. J. Phys.* **64**, 1168 (1986).
- ²⁴ G. Busse and H. G. Walther, in *Principles and Perspectives of Photothermal and Photoacoustic Phenomena*, Vol. 1, edited by A. Mandelis (North-Holland, New York, 1991), Chap. 5.
- ²⁵ M. Abramowitz and A. Stegun, *Handbook of Mathematical Functions*, 9th ed. (National Bureau of Standards, Washington, DC, 1970).
- ²⁶ F. A. McDonald, *J. Photoacoust.* **1**, 21 (1982).